COLO HEP 423

Search for Supersymmetry and the Two Photon Background

Nick Danielson
University of Colorado
Department of Physics

November 9, 1998

COLO HEP 423

Abstract

The Standard Model is the currently accepted model of particle physics. Supersymmetry is a theory that has been proposed to explain various problems with the Standard Model. If Supersymmetry theory is accurate, there are many Standard Model processes that may overwhelm Supersymmetric signals. In particular, the Standard Model two photon process may pose a large problem for the discovery of some of the Supersymmetric signals. Techniques that can be used to find Supersymmetry and to measure the masses of Supersymmetric particles are discussed. In particular, methods are developed for reducing the two photon background while leaving the signal of the Supersymmetric electron unchanged. This signal can then be used to determine the masses of various Supersymmetric particles. These methods were developed by using Monte Carlo simulations of both Standard Model and Supersymmetric data in an e^+e^- linear collider running at an energy of 500 GeV.

Contents

1 Introduction

The currently favored theory of particle physics is known as the Standard Model. However, it does not explain all of particle physics adequately, and many theorists are now looking at possible theories of physics beyond the Standard Model. One such theory is known as Supersymmetry. This paper will focus on techniques for discovering Supersymmetry by discerning between Standard Model processes and Supersymmetric processes. In particular, the Standard Model process known as the two photon process may pose a problem for the search for Supersymmetry, and this will be the emphasis of most of this thesis. However, before discussing this, I will present a summary of the Standard Model, an explanation of some of the motivation behind Supersymmetry and a summary of what Supersymmetry actually predicts. This background information is followed by a description of one particular Supersymmetric process known as the selectron process. I explain how the signal from this process can be overwhelmed by the Standard Model two photon process and I mention some techniques that can be used to reduce this background. Lastly I use these techniques to demonstrate how the masses of Supersymmetric particles could be measured if Supersymmetry is an accurate description of nature.

2 The Standard Model

Since the discovery of the electron in 1897, experiments have revealed a multitude of subatomic particles. By the 1970s, physicists were doubtful that all these particles were fundamental in the sense that they could not be broken down into smaller particles. A theory called the Standard Model emerged which incorporated all the then-known particles as well as predicted the existence of new particles which have since been discovered. In addition, it helps explain three of the fundamental forces of nature—the electromagnetic, weak, and strong forces.

On the scale of the very small, particles behave as if they have an intrinsic angular momentum quantum number, or "spin" which comes only in either integers or half-integers. If a particle has an angular momentum quantum number of $\frac{1}{2}$ or 1, we say the particle is a spin 1/2 particle or spin 1 particle, respectively. We call particles with half-integer spin "fermions" and particles with integer spin "bosons." It turns out that fermions and bosons have very different properties. Fermions make up matter and bosons are the particles which carry the forces that cause interactions between fermions. Table 1 lists the fundamental particles predicted by the Standard Model. All of these particles have been detected by experiment. In addition to the particles listed in Table 1, there is one more particle posited to exist—the Higgs particle. By itself, the Standard Model predicts that all particles are massless. With the addition of the Higgs particle—or perhaps many kinds of Higgs particles—the Standard Model explains the existence of mass. This last particle, the Higgs, has not been discovered, and there are currently many searches for it.

Table 1: The fundamental particles predicted by the Standard Model. The existence of all these particles has been confirmed by experiment.

Fermions (Half-Integer Spin)		**Bosons (Integer Spin)**
Leptons	Quarks	Carrier Bosons
e, ν_e	u, d	γ, W, Z^0, g
μ, ν_μ	c, s	
τ, ν_τ	t, b	

Despite the Standard Model's great success in explaining experiments in particle physics, there are a number of hints that there is some kind of physics beyond the Standard Model. For instance, the mass of the Higgs is predicted to be infinite, which surely is unphysical. Also, the fundamental forces of nature are associated with "coupling constants" that determine the forces' strengths. These coupling constants depend on energy, and at high energies ($\approx 10^{23}$ eV) they don't quite assume the same value. If they were to assume the same value, this would suggest that at high energies these forces are different aspects of one force, which is aesthetically very pleasing. This hints that perhaps the Standard Model is almost, but not quite, complete.

3 Supersymmetry

One of the leading theories of physics beyond the Standard Model is Supersymmetry [1], [2]. Supersymmetry predicts that each boson has a Supersymmetric partner that is a fermion and that each fermion has a Supersymmetric partner that is a boson. Figure 2 shows the Standard Model particles and their Supersymmetric partners. Thus Supersymmetry predicts the existence of many new particles which have not been detected. The introduction of these particles causes the mass of the Higgs to become finite. In addition, it has been shown that with the addition of Supersymmetry the coupling constants do, in fact, take on the same value within their experimental uncertainties at high energies. It should be noted that in order for this unification of the coupling constants to occur, theorists have shown that the mass scale of the Supersymmetric particles must be on the order of 1 TeV [3]. Thus if colliders running much past this energy do not detect Supersymmetry, much of the motivation for Supersymmetry will be gone. In addition, this may explain why none of the predicted particles have been discovered yet. Current colliders have not searched much higher than 80 GeV (=0.08 TeV).

Table 2: Standard Model particles and their Supersymmetric partners.

Standard Model	Supersymmetry
e^-, ν_e	$\widetilde{e}^-_{L,R}$, $\widetilde{\nu}_e$
μ^-, ν_μ	$\widetilde{\mu}^-_{L,R}$, $\widetilde{\nu}_\mu$
τ^-, ν_τ	$\widetilde{\tau}^-_{L,R}$, $\widetilde{\nu}_\tau$
u, d	$\widetilde{u}_{L,R}$, $\widetilde{d}_{L,R}$
c, s	$\widetilde{c}_{L,R}$, $\widetilde{s}_{L,R}$
t, b	$\widetilde{t}_{1,2}$, $\widetilde{b}_{1,2}$
γ, Z^0	$\widetilde{\chi}^0_1$, $\widetilde{\chi}^0_2$, $\widetilde{\chi}^0_3$, $\widetilde{\chi}^0_4$
g	$\widetilde{g}$
W^+	$\widetilde{\chi}^+_1$, $\widetilde{\chi}^+_2$

There are slightly different versions of Supersymmetric theory. The version used for the studies discussed in this paper is called the Minimal Supergravity model. For this model there are five defining parameters: m_0, $m_{1/2}$, A_0, $\tan\beta$, and $\mathrm{sgn}(\mu)$. The physical meanings of these parameters are beyond the scope of this paper, but the important point is that different values for these parameters give slightly different manifestations of Supersymmetry. For instance, the masses of particles and the ease with which various particles can be created will vary according to the values of these parameters. Because the details of Supersymmetry cannot be known unless Supersymmetric particles are actually discovered, theoreticians have given us five points in this parameter space to study. These points by no means reflect every possible version of Supersymmetry, but they have been designed to encompass a large portion of the possible range of Minimal Supergravity's parameters. Table 3 shows the values of the parameters for the various points, and Table 4 lists the masses of various Supersymmetric particles in each of the five points.

Table 3: Values of the parameters for the five points. Point 4 is a non-supergravity point and has different parameters.

	m_0	$m_{1/2}$	A_0	$\tan\beta$	$\mathrm{sgn}(\mu)$	
Point 1	400	200	0	2	-1	
Point 2	100	300	0	2	-1	
Point 3	200	100	0	2	-1	
Point 5	300	130	-600	2	+1	
	$m_{\tilde{g}}$	$m_{\tilde{q}}$	$m_{\tilde{\ell}_i}$	$\tan\beta$	μ	m_A
Point 4	900	1000	1000	10	-100	200

According to the Mimimal Supergravity model, a quantity called R-parity[1] could be conserved. This conservation law is necessary to avoid proton decay which is not observed in nature. This requires that Supersymmetric particles be produced in pairs and that a Supersymmetric particle must decay into another Supersymmetric particle and a Standard Model particle. This implies that in this model the lowest mass Supersymmetric particle is stable. In this model, the lightest Supersymmetric particle is denoted $\tilde{\chi}_1^0$ and is called the neutralino. All other Supersymmetric particles have a short lifetime and decay eventually into the lowest mass Supersymmetric particle, which unfortunatly interacts only through the weak force, much like neutrinos. Thus it is invisible to our detectors. So one of the major signs that a Supersymmetric event has taken place is large amounts of missing energy and momentum.

4 Methods used

Currently, no experiments have turned up evidence for Supersymmetric particles, but there are plans to build particle accelerators that run at higher

[1] R-parity is defined as $(-1)^{3B+L+2S}$ where B is baryon number, L is lepton number, and S is strangeness.

Table 4: Various particle masses for points 1–5.

	Point 1	Point 2	Point 3	Point 4	Point 5
$\widetilde{\chi}_1^0$	86.05	128.70	44.52	77.83	57.17
$\widetilde{\chi}_2^0$	175.45	257.22	97.00	115.29	111.46
$\widetilde{\chi}_3^0$	492.70	535.50	256.94	146.84	444.77
$\widetilde{\chi}_4^0$	501.75	542.54	273.64	292.41	464.60
$\widetilde{\chi}_1^\pm$	175.34	257.20	96.39	96.06	110.10
$\widetilde{\chi}_2^\pm$	500.81	542.24	272.04	292.46	461.60
h^0	83.25	89.92	68.29	126.96	101.42
H^0	745.30	681.40	378.99	201.61	622.61
A^0	741.05	676.41	371.09	200.00	620.01
$H^\pm$	744.61	680.33	378.49	214.81	624.10
$\widetilde{\nu}_L$	421.40	230.02	206.62	1000.00	314.60
$\widetilde{e}_L^\pm$	425.92	238.21	215.70	1000.00	320.64
$\widetilde{e}_R^\pm$	408.80	156.95	206.54	1000.00	307.45
$\widetilde{t}_1$	424.43	535.82	263.71	924.84	150.66
$\widetilde{b}_L$	520.57	621.86	274.27	1000.00	380.76
$\widetilde{q}_L$	603.27	668.38	316.73	1000.00	462.49
$\widetilde{t}_2$	550.61	656.48	329.48	1096.29	494.73
$\widetilde{b}_R$	595.55	653.10	312.97	1000.00	456.58
$\widetilde{q}_R$	603.27	668.38	316.73	1000.00	462.49
$\widetilde{t}_2$	550.61	656.48	329.48	1096.29	494.73
$\widetilde{b}_R$	595.55	653.10	312.97	1000.00	456.58
$\widetilde{q}_R$	603.27	668.38	316.73	1000.00	462.49
$\widetilde{g}$	550.62	759.04	298.40	900.00	425.52

energies that will explore physics beyond the Standard Model. For instance, there currently is an effort to design a collider known as the Next Linear Collider (NLC) which will run at center of mass energies of approximately 500–1500 GeV.[2] If built, this collider will further test the predictions of the Standard Model by studying, for instance, the top quark and the W boson. In addition, it will look for physics beyond the Standard Model such as Su-

[2] 1 GeV= 10^9 eV. One eV is the energy an electron gains by "falling" through a potential difference of one volt.

persymmetry. In order for Supersymmetry to be discovered, we must know what signs to look for.

By using Monte Carlo simulations, we can develop techniques for finding Supersymmetry. We also can figure out what features a new linear collider and detector will need in order to see Supersymmetry. In order to do this, we simulate both Standard Model and Supersymmetric data. We use the programs ISAJET, PYTHIA, Guinea Pig, and HERWIG [4], [5], [6]. We then apply "cuts" to these data. A cut is a rule for eliminating certain events that is designed to reduce unwanted background events while leaving the desired signal events alone. For instance, the signature of a Supersymmetric electron (selectron) event is exactly two visible particles: one electron and one positron. If we wish to study these events, we apply a cut and look only at events with exactly one electron and one positron.

Table 5 shows the cross-sections[3] of the Standard Model processes we have studied, while Table 6 shows the cross-sections of various Supersymmetric processes. Figure 1 shows how the Standard Model cross-sections vary with center of mass energy ($\sqrt{s}$). All the data discussed in this paper represent collisions at a center of mass energy of 500 GeV. In addition, we allow the electron beam to have 80% right or left polarization.[4] After the events are generated, we send them through a routine that smears the data to simulate a detector's resolution and inefficiencies. One important inefficiency that is simulated is the finite size of the beam pipe. In a typical collider, the two colliding particles travel down a beam pipe to the interaction region and collide, creating new particles. If one of the particles travels at a small angle to the beam axis (the z-axis), it may go down the beam pipe undetected. Thus any detector will have some smallest angle that it can see down to. Unless indicated otherwise, all the studies in this paper assume a detector that can see down to $\cos\theta = .995$ (≈ 100 mrad).

[3]The cross-section (σ) of a process is a measurement of the production probability of the process, with more common processes having higher cross-sections. All the cross-sections in this paper are measured in femtobarns (fb).

[4]An electron can have its spin axis pointing along or against its direction of motion. This is referred to as its polarization. "80% right polarization" means 90% of the electrons have their spin axis pointing along the direction of motion, and 10% pointing opposite the direction of motion.

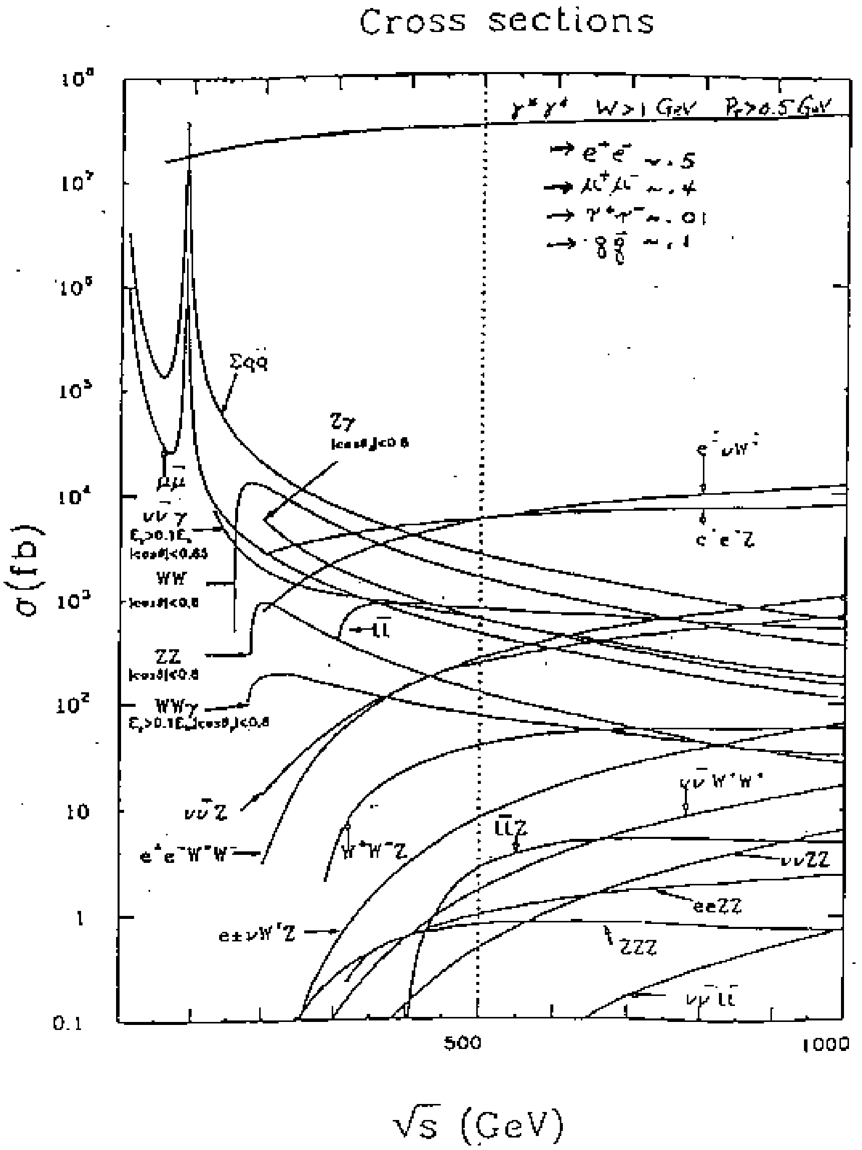

Figure 1: The cross-sections of various Standard Model backgrounds as a function of energy. $\sqrt{S}$ refers to the center of mass energy.

Table 5: Cross-sections (in fb) for various Standard Model processes at 500 GeV.

Process	Cross-section (fb)	
	80% Left	80% Right
$e^+e^-\gamma^*\gamma^*$	4.42×10^7	4.42×10^7
$\rightarrow e^+e^-e^+e^-$	2.76×10^7	2.76×10^7
$\rightarrow e^+e^-\mu^+\mu^-$	1.24×10^7	1.24×10^7
$\rightarrow e^+e^-$hadrons	3.93×10^6	3.93×10^6
$\rightarrow e^+e^-\tau^+\tau^-$	3.09×10^5	3.09×10^5
$\rightarrow e^+e^-W^+W^-$	111	111
$\gamma\gamma$	6840	6840
γ^* or Z^0	5380	5380
$\gamma\gamma^*$ or Z^0	5200	5200
Z^0Z^0	427	427
W^+W^-	12710	1461

Table 6: Cross sections (in fb) for various point 2 production modes at 500 GeV. In this table, $\widetilde{\ell}=\widetilde{\mu}+\widetilde{\tau}$. This data was generated with ISAJET [4].

	500 GeV	
	80% Left	80% Right
$\widetilde{\chi}_1^0\widetilde{\chi}_1^0$	65	404
$\widetilde{\chi}_1^0\widetilde{\chi}_2^0$	63	7
h^0Z^0	70	54
$\widetilde{\nu}_e\overline{\widetilde{\nu}}_e$	121	16
$\widetilde{e}_L^+\widetilde{e}_L^-$	7	2
$\widetilde{e}_R^+\widetilde{e}_R^-$	53	317
$\widetilde{e}_L^\pm\widetilde{e}_R^\mp$	145	146
$\widetilde{\ell}_R^+\widetilde{\ell}_R^-$	25	75
$\widetilde{\ell}_L^+\widetilde{\ell}_L^-$	50	150
Total	590	1104

5 The selectron

In this section I will describe one very important Supersymmetric process—the Supersymmetric electron, or selectron ($\widetilde{e}^\pm$) process—whose signal, it turns out, seems to be overwhelmed by the Standard Model two photon process. In the section following this, I will discuss ways of minimizing the two photon events while keeping the selectron signal.

As Table 4 shows, there are two selectrons, each with a different mass: the left-handed selectron ($\widetilde{e}_L$) and the right-handed selectron ($\widetilde{e}_R$). Thus there are four different selectron production modes: $\widetilde{e}_L^+\widetilde{e}_L^-$, $\widetilde{e}_L^+\widetilde{e}_R^-$, $\widetilde{e}_R^+\widetilde{e}_L^-$, and $\widetilde{e}_R^+\widetilde{e}_R^-$. The cross-sections for these processes change depending on the beam polarization as Table 6 reveals. The selectron always decays into an electron and a neutralino ($\widetilde{\chi}_1^0$). The $\widetilde{\chi}_1^0$ escapes undetected, so the selectron signal is exactly two visible particles: one electron and one positron, and missing energy. A "visible" particle is a particle that makes it to the detector.

Before discussing the kinematics of this process, I will discuss the kinematics of a simpler process: a reaction of the form $e^+e^- \to A + \overline{A}$ where $A \to C + D$. In this reaction, $\overline{A}$ denotes the anti-particle of A, so A and $\overline{A}$ have the same mass. Figure 2 is a graphical representation of this. If we were to look at a histogram of the energy of particle C, we would find clear low and high energy endpoints. The most energy particle C can have is when it travels in the same direction as particle A. Similarly, the least energy particle C can have is when it travels opposite particle A's direction. Appendix A shows the calculations behind this and further reveals that particle C's energy should be evenly distributed, i.e. the histogram should have a box shape. By measuring the endpoints of the box distribution, the masses of particle A and D can be determined.

The selectron process is slightly more complicated than this due to the fact that the $\widetilde{e}_R$ and $\widetilde{e}_L$ have different masses, whereas particle A and $\overline{A}$ had the same mass. It turns out[5] that in this case we expect to see a superposition of several box shapes. Figure 3 and Figure 4 show this phenomenon. By looking at the energy endpoints of the electrons and positrons in selectron events, the masses of the $\widetilde{\chi}_1^0$ and $\widetilde{e}^\pm$ can be determined. Note the difference between left and right polarized events. This tells us that by changing beam polarization, we can change the relative sizes of the boxes. This is important because there is no Standard Model signal whose height depends on beam polarization in this manner. The selectron process is, therefore, a key Supersymmetric signal.

[5]See appendix A.

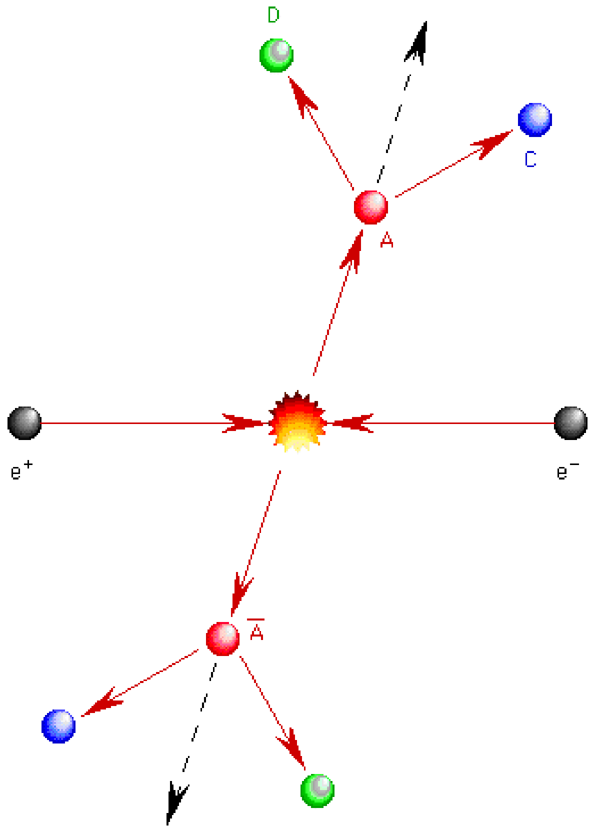

Figure 2: A reaction of the form $e^+e^- \to A + \overline{A}$ where $A \to C + D$. The incoming electron and positron (black) annihilate and create an $A\overline{A}$ pair which decay into C and D. The dotted line indicates the direction C would have to travel in order to have its maximum energy.

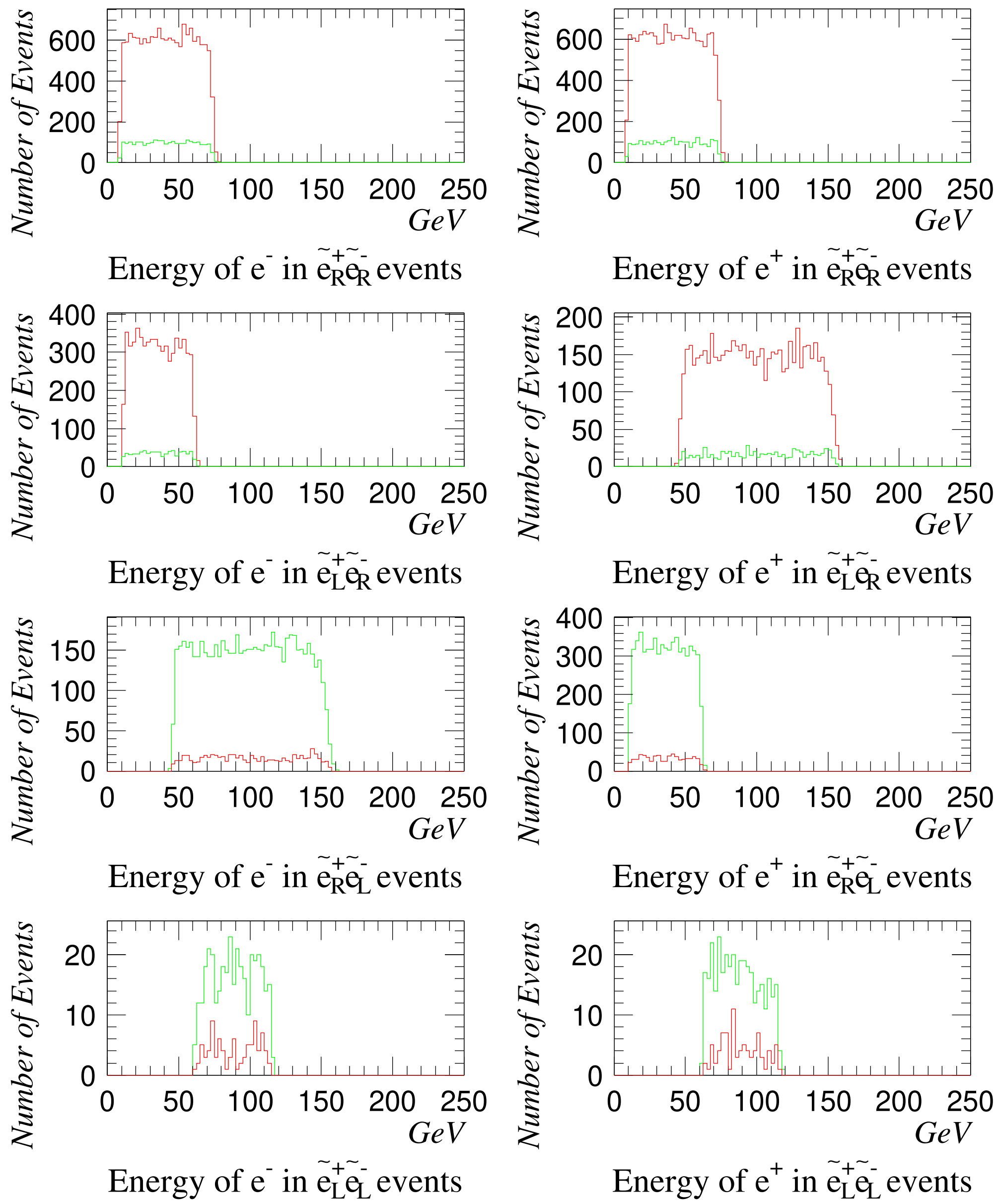

Figure 3: The energy distribution of electrons and positrons that come from the various selectron production modes. The 80% right polarized data is red, the 80% left polarized data is green. This data represents 50 fb^{-1} of data.

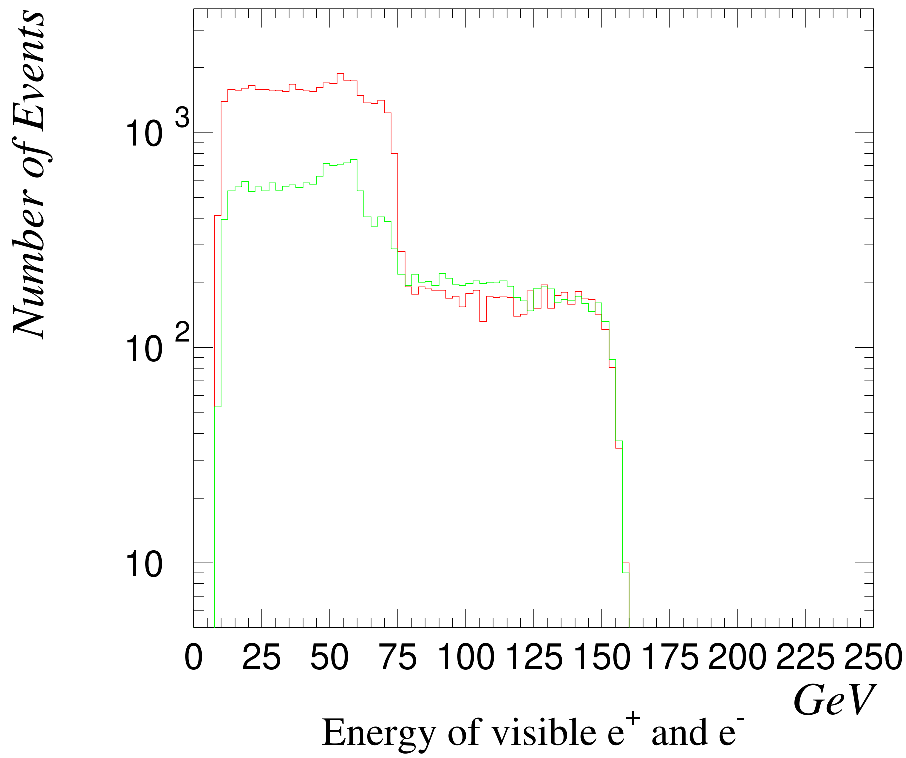

Figure 4: The energy distribution of electrons and positrons that come from selectron events. This is the sum of all the plots in Figure 3. The 80% right polarized data is red while the 80% left polarized data is green. This data represents 50 fb^{-1} of data.

6 The two photon process

Figure 1 shows that one major source of Standard Model background is the two photon ($\gamma^*\gamma^*$) process, which is approximately three orders of magnitude larger than most other Standard Model background processes at 500 GeV and therefore four to five orders of magnitude larger than the Supersymmetric signals. All our $\gamma^*\gamma^*$ data was simulated with a Monte Carlo program called HERWIG [5] at an energy of 500 GeV with no electron polarization, since polarization doesn't affect two photon events. The emphasis of this paper is the two photon process $e^+e^- \to e^+e^-\gamma^*\gamma^* \to e^+e^-e^+e^-$. Figure 5 shows the lowest order feynman diagram for this process. This is the process that HERWIG simulates. In addition, there are many higher order processes which HERWIG does not simulate. Figure 6 illustrates several of these. These processes will most likely have a smaller, yet still measurable, effect on Supersymmetry studies.

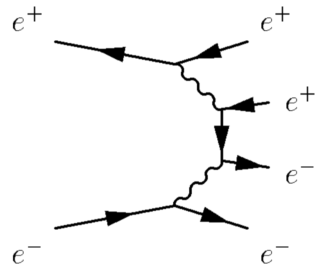

Figure 5: The production of lowest order $\gamma^*\gamma^*$ events.

A typical $\gamma^*\gamma^*$ event consists of a "collision" in which the initial electron and positron scatter slightly and some of their energy and momentum is used to produce new particles—in our case a new electron-positron pair. These events are similar to Rutherford scattering[6] in that the scattered electron and positron tend to be deflected only slightly. This means that they often travel down the beam pipe and thus leave the detector unseen, taking energy and momentum with them. The other electron and positron tend to be low energy and tend to be visible. Figure 7 is a histogram of the number of visible particles in $\gamma^*\gamma^*$ events. Very few events have all four electrons visible. As mentioned above, missing energy and momentum are precisely the signs that Supersymmetry would leave. In particular, $e^+e^- \rightarrow \gamma^*\gamma^*\ e^+e^- \rightarrow\ e^+e^-e^+e^-$ closely mimics the selectron signal mentioned above in Section 5 because these events often have exactly two visible particles: one electron and one positron. So not only are $\gamma^*\gamma^*$ events very numerous at high energies, they are also sufficiently similar to Supersymmetric events to cause problems for detecting Supersymmetry.

[6] Rutherford scattering refers to the scattering of α-particles (a ^{4}He nucleus) off of an atomic nucleus. The differential cross-section is proportional to $1/\sin^4\frac{\theta}{2}$ indicating that the α-particles are most often scattered only slightly, at low angles.

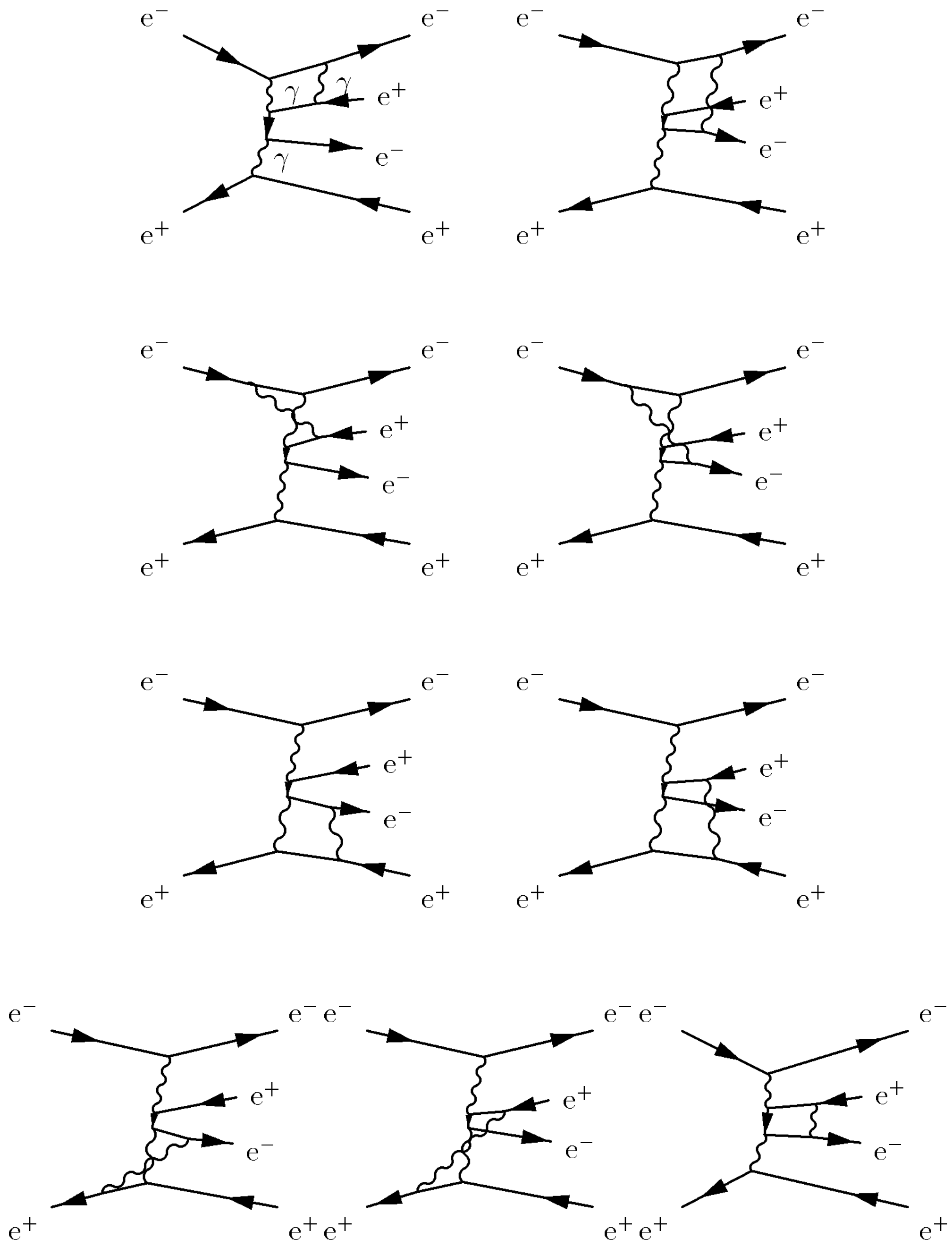

Figure 6: Next-to-lowest-order $\gamma^*\gamma^*$ processes.

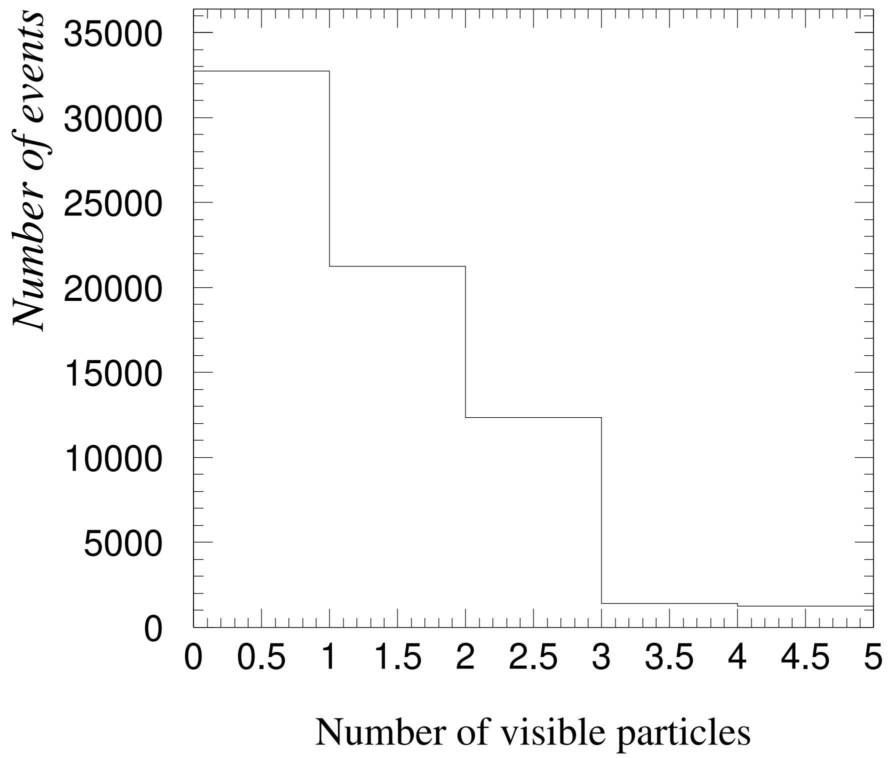

Figure 7: The number of visible particles in $\gamma^*\gamma^*$ events.

6.1 The standard cuts

We have assumed that the linear collider running for one year would produce 50 fb^{-1} of data. At this luminosity and at 500 GeV, point 2 predicts approximately 23,000 selectron events. However, we expect 2×10^9 two photon events. Unfortunately, our computers do not have enough disk space to store this many events so we must make a few "standard cuts" on our data in order make the number of events manageable. These cuts were designed to eliminate other Standard Model background events such as W^+W^- background while preserving Supersymmetric signals. These standard cuts (and other cuts) are discussed in detail in [7]. Here is a brief summary:

1. Require all events to have exactly two visible particles: one electron and one positron. As mentioned earlier, nearly all selectron events will pass this cut. However, many Standard Model events (including $\gamma^*\gamma^*$

events) will be eliminated by this cut.

2. Require all events to have less than 1 GeV of energy in the region $100\,\text{mrad} < |\theta| < 451\,\text{mrad}$[7]. Many Standard Model backgrounds such as the W^+W^- background are very forward, with the decay products traveling at low angles to the z-axis. This cut removes many of these events, leaving most of the Supersymmetric events alone.

3. The energy in the most energetic hemisphere must be less than $.4E_{cm}$ where E_{cm} is the center of mass energy—in our case, 500 GeV. The most energetic hemisphere is defined by dividing the reaction into two. The half with the most energy deposited in it is the most energetic hemisphere. Normally we would expect about 1/2 E_{cm} in each hemisphere, but since Supersymmetric particles are not visible we expect less than this.

Once these cuts have been applied to our $\gamma^*\gamma^*$ data, the number of events is reduced by a factor of about 20 to about 9×10^7. This is still too many events to store on disk, so we ran less than this number and scaled the data by a factor of 150.[8]

6.2 Transverse Momentum

One feature of $\gamma^*\gamma^*$ events that distinguishes them from many other kinds of events is their total transverse momentum (p_t). An event's total transverse momentum is defined as

$$p_t^2 = (\sum_i p_{x,i})^2 + (\sum_i p_{y,i})^2$$

where i runs over all the visible particles in the event and $p_{x,i}$ and $p_{y,i}$ refer to the momentum in the x and y direction for the ith particle. The positive z direction is defined as the direction of the incident e^-. In this case there are only two visible particles: an electron and a positron. As mentioned above, in $\gamma^*\gamma^*$ events the scattered high energy electron and positron tend to be in the forward direction with a small angle relative to the z-axis. This means

[7]Or $.90 < |\cos\theta| < .995$.

[8]This is a large factor, but is better than scaling by a factor of several thousand, which is what we would have to do if no standard cuts had been made.

that they tend to carry very little momentum in the x and y directions, so their transverse momentum is usually close to zero. The initial incoming electron and positron have equal and opposite momentum, so conservation of momentum implies that the momentum of the outgoing four particles must add to zero. This means that a plot of the magnitude of the total visible transverse momentum must be the same as a plot of the magnitude of the total *in*visible transverse momentum and should be peaked at zero. On the other hand, selectron events do not tend to be forward, so their transverse momentum will not be peaked at zero. Figure 8 is a histogram of the total transverse momentum of $\gamma^*\gamma^*$ and selectron events. As expected, the $\gamma^*\gamma^*$ events are peaked at zero, while the selectron events are spread out over a larger range. By adding a cut requiring all events to have more than a certain value of p_t, we can eliminate much (or even all) of the $\gamma^*\gamma^*$ background. Figure 9 shows the energy distribution of electrons and positrons in both selectron and $\gamma^*\gamma^*$ events as the p_t cut is varied. When the total p_t cut is set at 40 GeV/c, most of the $\gamma^*\gamma^*$ background is removed. This cut also removes those selectron events where the electron/positron energy is low. The problem with this cut is that most of the difference between right and left polarized selectron events is at low p_t, so by eliminating low p_t events, we are minimizing an effect that is one of the main motivations for studing selectron events. This can be seen in Figure 9. In the first plot there is a large difference between right and left data, but by the last plot, the difference is much smaller. However, the energy endpoints are well-preserved, so a mass measurement could be accomplished after this cut. Ideally, though, we would like to remove $\gamma^*\gamma^*$ events without using such a high p_t cut.

6.3 Seeing particles at small angles

The only reason $\gamma^*\gamma^*$ events pose a problem for selectron studies is that our detector is inefficient and can't see particles with small angles. If we could see one of the two high energy particles that travel down the beam pipe, we would see three or four particles and could eliminate all the $\gamma^*\gamma^*$ backgroud for selectron events without having to use a p_t cut. How small an angle must a detector be able to see in order to substantially reduce this $\gamma^*\gamma^*$ background?

One way to determine the answer is to look at the electron and positron that went down the beam pipe and choose the one with the largest angle. If our detector could see this particle, we would be able to cut the event.

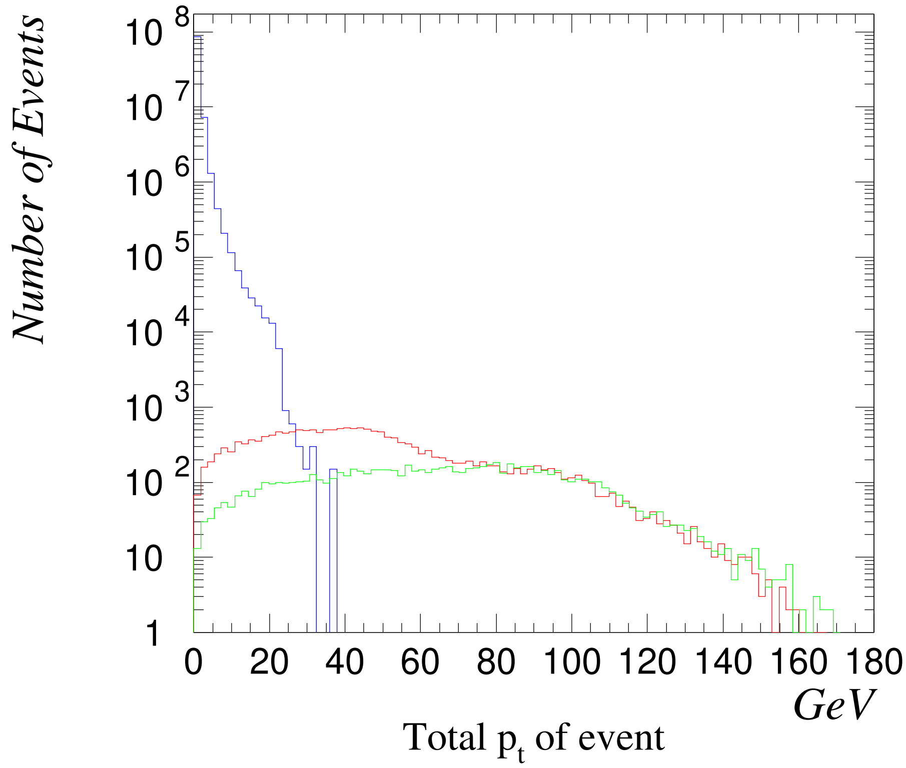

Figure 8: The total transverse momentum of $\gamma^*\gamma^*$ events (blue) and selectron events (red for 80% right polarized data, green for 80% left polarized data). This represents 50 fb^{-1} of data.

Figure 10 is a histogram of the angle of this high angle particle as the p_t cut is varied. The figure indicates that if our detector can see down to 40 mrad, then a p_t cut of 10 or 15 GeV/c could eliminate most of the $\gamma^*\gamma^*$ background.

7 Mass determination

After assuming our detector can see down to 40 mrad, and after the three standard cuts and the cut requiring $p_t > 15$ GeV/c cut, the energy distribution of electrons and positrons looks as in Figure 11 when the Standard Model backgrounds mentioned in Table 5 are included with the two photon background. The energy endpoints have not changed significantly, so the masses

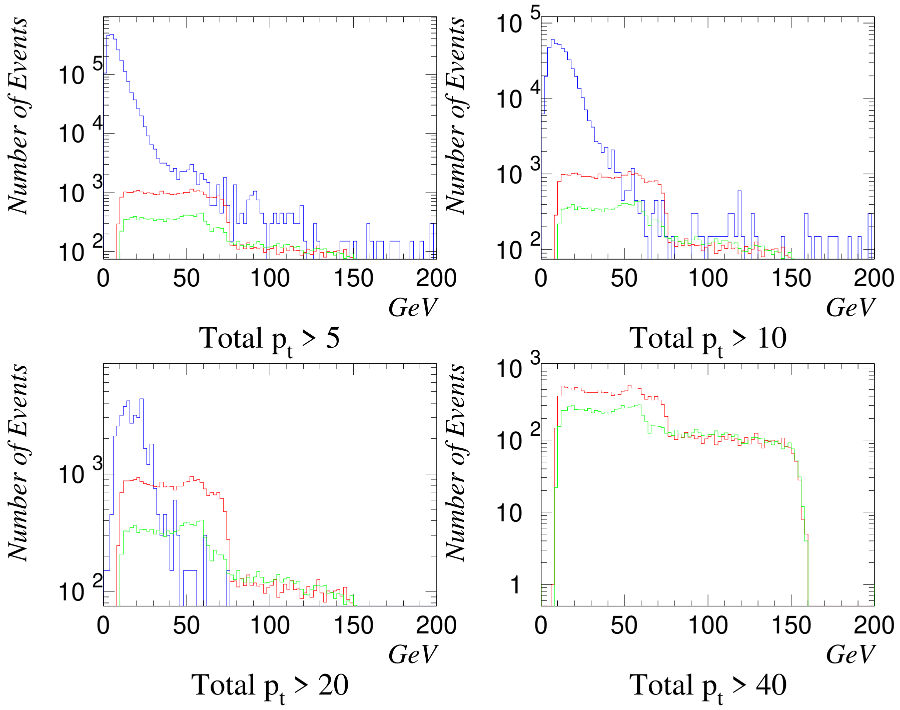

Figure 9: The energy of electrons and positrons as the cut on total transverse momentum is varied. The 80% right polarized selectron data is red, the 80% left polarized data is green, and the $\gamma^*\gamma^*$ data is blue. This represents 50 fb^{-1} of data.

of the $\widetilde{\chi}_1^0$ and $\widetilde{e}^{\pm}$ can be determined. Using a computer-generated best fit to this box distribution yields the endpoints: E_{min}=9.005 GeV, E_{middle}=73.33 GeV, and E_{max}=153.4 GeV. The equations described in Appendix A allow us to calculate the masses which are listed in Table 7. The calculated masses agree well with the "known" masses which were initially input into the Monte Carlo simulation. So despite the large cross-section of the two photon process, the endpoints can be seen well enough to determine the Supersymmetric particles' masses.

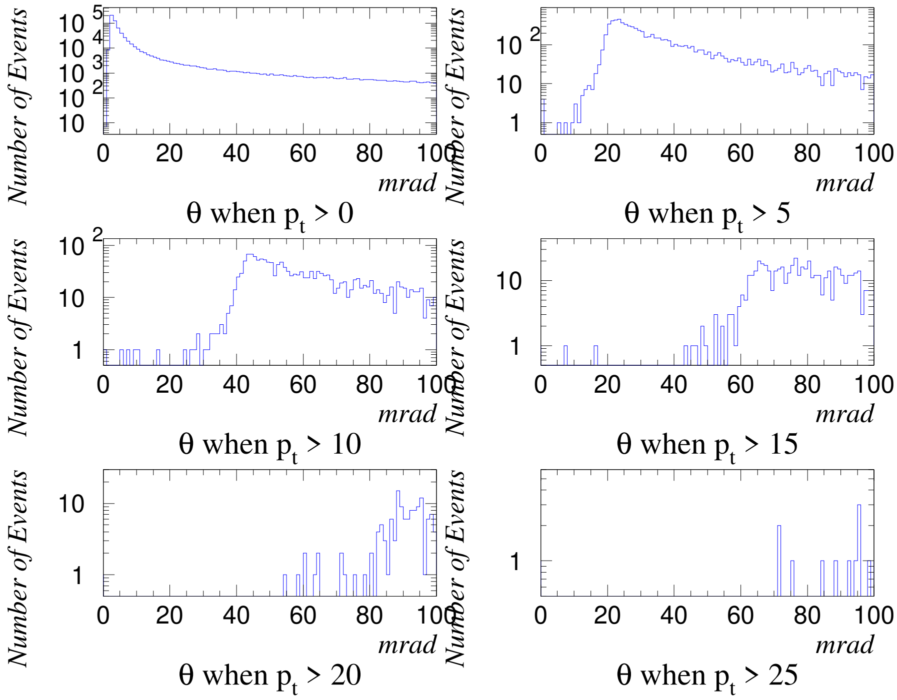

Figure 10: The angle (in mrad) of the particle with the largest angle that went down the beam pipe. Each plot corresponds to a different p_t cut. This represents only .33 fb^{-1} of two photon data.

Table 7: The masses of Supersymmetric particles (in GeV/c^2) calculated using the endpoints in Figure 11.

Particle	Known Mass	Measured Mass	Discrepancy
$\widetilde{\chi}_1^0$	129	128	0.7 %
$\widetilde{e}_R$	157	156	0.6 %
$\widetilde{e}_L$	238	236	1.1 %

8 Conclusions

Supersymmetry is currently a leading candidate for physics beyond the Standard Model. If Supersymmetry proves to be an accurate description of na-

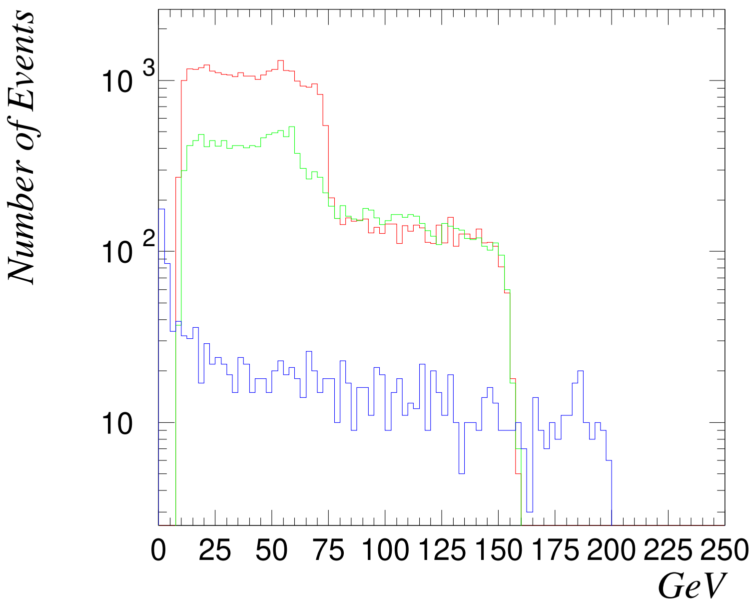

Figure 11: The energy of electrons and positrons after standard cuts, a 15 GeV/c p_t cut, and assuming a detector that sees down to 40 mrad. This includes the other Standard Model backgrounds mentioned in Table 5. Red is 80% right polarized selectron events, green is 80% left polarized selectron events, and blue is Standard Model events. This represents 50 fb^{-1} of data.

ture, the selectron process may be an important signal because of the way its cross-section depends on beam polarization, at least in the mSUGRA model. The two photon process has a very large cross-section and can drown out many Supersymmetric signals, including the selectron signal. For this reason, it should be studied further, and more accurate simulations of this process need to be developed since our current simulations only simulate lowest order processes.

The signal for Supersymmetry is missing energy and momentum. Standard Model events such as the two photon process can mimic this signal by having particles travel down the beam pipe. Because of this, it appears that a detector that can see down to very small angles would be beneficial to the search for Supersymmetry. Finally, a method similar to the endpoint method of mass determination may be applicable for measuring the masses of Supersymmetric particles.

Appendix A: Mass and endpoint calculations

We would like to consider a reaction as shown in Figure 2. In our case, the two selectrons have different masses, so we would like to allow the mass of A to differ from the mass of $\overline{A}$. To avoid confusing particle A and particle $\overline{A}$, I will call particle $\overline{A}$ particle B. We would like to obtain an expression for M_A, M_B, and M_D by knowing the low and high energy endpoints of C and by knowing M_C.

We first consider the decay of A into C and D in the rest frame of A. Conservation of momentum tells us that $p_C^2 = p_D^2$. Then, if we use Einstein's energy relation[9]: $E^2 = m^2 + p^2$ and conservation of energy, we obtain

$$E_A = E_C + E_D$$

$$M_A = E_C + \sqrt{M_D^2 + P_D^2} = E_A + \sqrt{M_D + P_C^2}$$

$$M_A = E_C + \sqrt{M_D + E_C^2 - M_C^2}$$

Solving for E_C yields

$$E_C = \frac{M_A}{2}\left[1 - \frac{M_D^2 - M_C^2}{M_A^2}\right] \tag{1}$$

Again using Einstein's energy relation, we find C's momentum:

$$p_C = \frac{M_A}{2}\sqrt{\left[1 - \frac{M_D^2 - M_C^2}{M_A^2}\right]^2 - \frac{4M_C^2}{M_A^2}} \tag{2}$$

Equations 1 and 2 are expressions for the energy and momentum of C in A's rest frame. We would like to know the energy of C in the *laboratory's* rest frame. To find the energy of a particle in a new frame of reference, the Lorentz transformations are used. They tell us that the energy of C in the laboratory frame is

$$E_{lab} = \gamma E_C + \gamma\beta p_C \cos\psi$$

[9] I have set the speed of light, c, equal to one in order to simplify our work, as is customary.

where

$$\beta = \frac{p_A}{E_A} = \sqrt{1 - \frac{M_A^2}{E_A^2}}$$

(I have used Einstein's energy relation to put β in a more useful form),

$$\gamma = \frac{1}{\sqrt{1-\beta^2}}$$

and where ψ is the angle the particle makes with the direction of the boost. In our case, ψ is the angle (in A's rest frame) that particle C makes with the dotted line in Figure 2. I have used Einstein's energy relation to put β in a more useful form. When A decays, particle C is equally likely to travel in any direction, and so C will be equally distributed in all solid angles. Thus C will have a flat distribution in $\cos\theta$. But $\cos\theta$ is precisely what E_{lab} depends on, so the energy distribution of C will, in fact, be flat as claimed earlier. Furthermore, the maximum and minimum energy will occur when $\cos\theta = +1$ and $\cos\theta = -1$ respectively:

$$E_{max} = \gamma E_C + \gamma\beta p_C \tag{3}$$

$$E_{min} = \gamma E_C - \gamma\beta p_C \tag{4}$$

We must now calculate β and γ. Conservation of momentum in the lab frame tells us that $p_B^2 = p_A^2 = \sqrt{E_A^2 - M_A^2}$. So conservation of energy in the lab frame tells us

$$E_{cm} = E_A + \sqrt{M_B^2 + p_B^2} = E_A + \sqrt{M_B^2 + E_A^2 - M_A^2}$$

where E_{cm} is the center of mass energy of the collision (500 GeV in our case). Solving for E_A yields

$$E_A = \frac{M_B^2 - M_A^2 - E_{cm}^2}{2E_{cm}}$$

Plugging this into the expression for β given above reveals that

$$\beta = \sqrt{1 - \frac{4M_A^2}{E_{cm}^2}\frac{1}{(1+\frac{M_A^2-M_B^2}{E_{cm}^2})^2}} \tag{5}$$

and

$$\gamma = \frac{1}{\sqrt{1-\beta^2}} = \frac{E_{cm}}{2M_A}\sqrt{1+\frac{M_A^2-M_B^2}{E_{cm}^2}} \tag{6}$$

Equations 1, 2, 4, 3, 5 and 6 tell us how to calculate the energy endpoints if we know the masses of all the particles involved. For instance, these equations allow us to verify the box distributions in Figure 3. I have left the formula for the endpoints broken into pieces like this because when all the parts are put together, the expression takes up several lines but doesn't add any understanding to the problem. We wish to go one step further, however. We would like to calculate the masses of A, B, and D if we know all the endpoints involved. In order to do this, we need more information than just the minimum and maximum energy endpoints. Recall that the actual energy distribution is a sum of many box distributions. To make our calculation, we will assume that in addition to knowing the overall minimum and maximum endpoints, we know the maximum and minimum endpoints of the lowest energy box distribution (the first plot in Figure 3). By looking at Figure 11, we see that it is clearly possible to discern these endpoints. This box corresponds to the case in which $e^+e^- \to \tilde{e}_R^+\tilde{e}_R^-$, and thus this corresponds to a case in which $M_A = M_B$. This will allow us to calculate M_A, which we can then use to determine M_B by looking at the overall energy distribution's endpoints. In this case, γ and β can be simplified, and for the record the expressions for minimum and maximum energy can be written as

$$E_{min} = \frac{E_{cm}}{4}\left(\left[1-\frac{M_D^2-M_C^2}{M_A^2}\right] - \sqrt{1-\frac{4M_A^2}{E_{cm}^2}}\sqrt{\left[1-\frac{M_D^2-M_C^2}{M_A^2}\right]^2-\frac{4M_C^2}{M_A^2}}\right)$$

$$E_{max} = \frac{E_{cm}}{4}\left(\left[1-\frac{M_D^2-M_C^2}{M_A^2}\right] + \sqrt{1-\frac{4M_A^2}{E_{cm}^2}}\sqrt{\left[1-\frac{M_D^2-M_C^2}{M_A^2}\right]^2-\frac{4M_C^2}{M_A^2}}\right)$$

These equations refer only to box distributions generated by a process in which $M_A = M_B$.

We now must invert these equations to yield expressions for M_A and M_D in terms of E_{min} and E_{max}. Returning to the expressions for the minimum and maximum energy (eqations 3 and 4) we find that

$$E_{min}E_{max} = \gamma^2 E_C - \gamma^2\beta^2 p_C = E_C^2 + \gamma^2\beta^2 M_C^2$$

where I've used the fact that $p^2 = E^2 - m^2$ and $\gamma = 1/\sqrt{1-\beta^2}$. But we can use the equation $E_{min} + E_{max} = 2\gamma E_C$ to eliminate E_C, so

$$E_{min}E_{max} = \frac{(E_{min} + E_{max})^2}{4\gamma^2} + \gamma^2\beta^2 M_C^2$$

We can now plug in the values of β and γ given above in equations 5 and 6 (after remembering that $M_A{=}M_B$) and solve for M_A. After much algebra, we arrive at a quadratic equation in M_A^2:

$$\left(\frac{E_{min} + E_{max}}{E_{cm}}\right)^2 M_A^4 - (M_C^2 + E_{min}E_{max})M_A^2 + E_{cm}^2 M_C^2$$

The solution to this equation is

$$M_A^2 = \frac{(M_C^2 + E_{min}E_{max}) \pm \sqrt{(E_{min}^2 - M_C^2)(E_{max}^2 - M_C^2)}}{2(E_{min} + E_{max})^2/E_{cm}^2} \tag{7}$$

Note that for any set of endpoints, there are *two* possible masses for A. To understand this, consider the low energy endpoint. This endpoint occurs when particle C travels opposite the direction of particle A. The energy of C in A's rest frame is fixed by the masses of A, C, and D. When we transform C's energy into the lab frame, one of three things can happen. (1) The masses of the particles involved can be such that in the lab frame C just happens to be exactly at rest. This corresponds to the case in which the square root in equation 7 is zero. (2) C can be traveling very slowly in A's rest frame so that in the lab frame C appears to be traveling in the same direction as A. This is much like throwing a ball backwards off a moving truck. If you throw it slowly enough, it will it still will appear to be moving in the same direction as the truck to someone who is at rest. (3) C can be traveling fast enough in A's rest frame that in the lab frame C is moves opposite the direction of A. Thus if you are told that C has a certain low energy endpoint, in general there are two sets of masses that yield the endpoint, depending on whether case two or case three applies.

The mass of D can now be calculated. We can substitute E_C (equation 1) into the equation $E_{min} + E_{max} = 2\gamma E_C$ and solve for M_D:

$$M_D^2 = M_A^2\left[1 + \frac{E_{min} - E_{max}}{\gamma M_A} + \frac{M_C^2}{M_A^2}\right]$$

If we now substitute equation 6 for γ, we arrive at

$$M_D^2 = M_A^2\left[1 - \frac{2(E_{min}+E_{max})}{E_{cm}} - \frac{M_C^2}{M_A^2}\right] \tag{8}$$

which can be calculated since we now know the mass of A. So we can now calculate the masses of A and D if we are given energy endpoints of the box distribution that arises when $M_A = M_B$. In other words, by looking at the endpoints of the high box distribution on the left of Figure 11 we can calculate the masses of $\widetilde{e}_R$ and the $\widetilde{\chi}_1^0$. Now we would like to use the overall maximum energy endpoint on the far right of the figure to calculate the mass of B (the $\widetilde{e}_L$).

The far left endpoint was caused by $\widetilde{e}_R\widetilde{e}_R$ events, but the far right endpoint is caused by $\widetilde{e}_L\widetilde{e}_R$events. We can perform a similar analysis by examining the side of the reaction in Figure 2 that has particle B. Much of the work needed to analyze this side of the reaction is similar to the work we've just done. We can arrive at most of the necessary quantities simply by replacing the "A's" with "B's" in the analogous quantities above. For instance,

$$E_C = \frac{M_B}{2}\left[1 - \frac{M_D^2 - M_C^2}{M_B^2}\right]$$

$$p_C = \frac{M_B}{2}\sqrt{\left[1 - \frac{M_D^2 - M_C^2}{M_B^2}\right]^2 - \frac{4M_C^2}{M_B^2}}$$

$$\beta = \sqrt{1 - \frac{4M_B^2}{E_{cm}^2}\frac{1}{(1+\frac{M_B^2 - M_A^2}{E_{cm}^2})^2}}$$

$$\gamma = \frac{E_{cm}}{2M_A}\sqrt{1 + \frac{M_B^2 - M_A^2}{E_{cm}^2}}$$

And the general expression for E_{max} is given by equation 3, except now all the quantities refer to the box distribution on the far right instead of the one on the far left. By plugging our new values of β, γ, E_C, and P_C into equation 3 we arrive at a new equation that can be solved for M_B since all the other quantities are known. After much algebra we obtain a quadratic equation in M_B^2. For the record, the quadratic equation is:

$$\left[E_{cm} - 2E_{max}\right] M_B^4 +$$
$$\left[4E_{cm}E_{max} - 2E_{cm}^2 E_{max} + 2M_A^2 E_{max} + 2(M_D^2 - M_C^2)E_{max} - 2E_{cm}(M_D^2 - M_C^2)\right] M_B^2 +$$
$$2(M_D^2 - M_C^2)E_{cm}^2 E_{max} - 2M_A^2(M_D^2 - M_C^2)E_{max} + E_{cm}(M_D^2 - M_C^2)^2 = 0$$

This has two positive solutions, one of which can be ruled out by conservation of energy.

Thus all the masses can be calculated by looking at the endpoints of the energy distribution of particle C, which in our case is an electron or positron.

References

[1] S. Kuhlman *et al.*, *Physics and Technology of the Next Linear Collider*, BNL 52-502, Fermilab-PUB-96-112, LBNL-PUB-5425, SLAC Report 485, UCRL-ID-124160, submitted to the Snowmass '96 conference, p. 61. 1996.

[2] H. Baer *et. al.*, "Determination of Supersymmetric Particle ¡Cross Sections and Angular Distributions at a High Energy Linear Collider." in appendix of *Physics and Technology of the Next Linear Collider*, BNL 52-502, Fermilab-PUB-96-112, LBNL-PUB-5425, SLAC Report 485, UCRL-ID-124160, submitted to the Snowmass '96 conference, 1996.

[3] Bagger, J., Matchev, K., Pierce, D. "Precision corrections to supersymmetric unification." *Physics Letters B* **348**, 443–450, 1995.

[4] F. Paige, S. Protopopescu, in *Supercollider Physics*, p. 41, edited by D. Soper (World Scientific, 1986); H. Baer, F. Paige, S. Protopopescu, and X. Tata in *Proceedings of the Workshop on Physics at Current Accelerators and Supercolliders*, edited by J. Hewett, A. White, and D. Zeppenfeld (Argonne National Laboratory, 1993).

[5] Marchesini, G., Webber, B. R., Abbiendi G., Knowles I. G., Seymour M. H., and Stanco L. "HERWIG." *Computer Phys. Commun.* **67**, 465, 1992.

[6] Schulte, D. in Appendix A of "Study of Electromagnetic and Hadronic Background in the interaction region of the TESLA Collider." University of Hamburg, unpublished. 1996, http://www.slac.stanford.edu/ twmark/nlc/GUINEA_PIG/.

[7] Goodman, E. "The Search for the Supersymmetric Selectron." COLO HEP 398. April, 1998,